Towards Efficient Wireless Power Transmission for Implantable Devices Using Three-Coil Receivers and Metamaterial Lenses

Journal:	*IEEE Antennas and Wireless Propagation Letters*
Manuscript ID	AWPL-09-23-2141
Manuscript Type:	Original Manuscript
Date Submitted by the Author:	24-Sep-2023
Complete List of Authors:	Wong, Blake; University of Hawai'i at Manoa Iskander, Magdy; University of Hawai'i at Manoa, Hawaii Advanced Wireless Technologies Institute Yun, Zhengqing; University of Hawai'i at Manoa Xiao, Yuanzhang; University of Hawai'i at Manoa Clemens, Scott; University of Hawaii@ Manoa, Hawaii Advanced Wireless Technologies Institute
Keywords:	wireless power transmission, metamatrial lens, non-radiative inductive coupling

Towards Efficient Wireless Power Transmission for Implantable Devices Using Three-Coil Receivers and Metamaterial Lenses

Blake Wong, *Student Member, IEEE,* Magdy F. Iskander, *Fellow, IEEE,* Zhengqing Yun, *Senior Member, IEEE,* Yuanzhang Xiao, *Member, IEEE,* and Scott Clemens, *Student Member, IEEE*

***Abstract*— Efficient wireless power transfer (WPT) can reduce the charging time of implantable devices and potentially minimize heating effects that can severely damage the patient's tissues. This paper presents two methods to increase WPT efficiency: one using three orthogonal receiving coils and the other using metamaterial lenses. The simulation results show that the first method improves the power transfer efficiency by up to 15% under the effects of receiver rotation within the human body. For the second method, the simulation results show that incorporating a metamaterial lens to the three implantable orthogonal coils can further increase the total power transmission efficiency under rotation by 2 dB. Increasing the number of turns of Coils 2 and 3 in the three-coil arrangement achieved similar SAR values to the conventional single-coil receiver. Our simulation study shows that limiting the number of turns in each coil to 10 is optimal as it reduces weight and interference between coils.**

***Index Terms*—HFSS, metamaterial lens, multi-layered tissue model, non-radiative inductive coupling, three orthogonal coils**

I. INTRODUCTION

IN biomedical implants, efficient wireless power transfer (WPT) is crucial because it reduces the charging time of the implantable device and potentially minimizes heating effects that can severely damage the patient's tissue. Many factors affect the power transfer efficiency such as the separation distances between transmitting (Tx) and receiving (Rx) coils, angular and transpositional misalignment between coils, and power losses in human tissues [1]. Efforts have been made to address these issues. In [2]-[4], circular two- and three-dimensional (3D) omnidirectional transmitter and receiver structures are developed to mitigate the sharp decrease of transmitted power due to the self-rotational and distance-separating effects. However, these circular coil designs do not share the same shape as the rectangular titanium implantable units found in commercially available products. In [5]-[7], rectangular orthogonal coils are proposed but not for implantable devices and not operating at the frequency band used in the industry. In [8]-[17], applications of metamaterial lenses to improve the power transmission system are proposed such as increasing the separation distances between the Tx and Rx coils, adding a tunable lumped element for single slab metamaterials to operate at various frequencies and mitigating misalignment. In [18]-[19], a multi-layered tissue human body model is employed and the specific absorption rate (SAR) is calculated.

Limitations of these works include operating frequencies outside the frequency band used in the industry, no results on the effects of a metamaterial lens with a receiver housed in a titanium implantable unit which is embedded in a multi-layered tissue human body model.

This paper proposes two methods to increase WPT efficiency: one using three orthogonal receiving coils and the other using metamaterial lenses. Our 3D receiver coils are housed in a titanium shell, creating the implantable unit. The implantable unit is then placed in a multi-layered tissue human body model and operates at 40 kHz, within the frequency range found in the industry. We then examine the power transmission effects of incorporating a metamaterial lens with the implantable unit. We tune the metamaterial lens and compare the effectiveness of the lens to two other implantable receiver units without using metamaterial lenses. Lastly, we calculated the SAR values under effects of rotation of receiving coils. We test the practicality of implementing two additional orthogonal receiver coils and the effects of increasing the number of turns by comparing the SAR values in tissue to a standard single-coil receiving implantable device.

In Section II, we describe the system design of the 3D receiving orthogonal coils in part A, and the metamaterial lens in part B. Section III includes the simulation results for the 3D receiving orthogonal coil design in part A and the metamaterial lens integrated with the 3D receiving orthogonal coil design in part B. Part C includes the SAR calculations in tissue. Section IV summarizes our results and discusses our future work.

II. SYSTEM DESIGN

A. 3D Receiving Orthogonal Coils

The receiver (Rx) is composed of three orthogonal coils placed inside the titanium shell. The dimensions of the coils are shown in Fig. 1. Coil 1 is vertical (facing front and back)

This work was supported in part by the U.S. National Science Foundation under Grant 1822213.The authors are with Hawaii Advanced Wireless Technologies Institute at the University of Hawaii, Manoa, Honolulu, HI, USA (correspondence e-mail: magdy.iskander@gmail.com)

and is facing the transmitting coil; Coil 2 is horizontal (facing up and down); and Coil 3 is vertical (facing left and right). The coils are wound by copper wires with a cross-sectional area of 0.1mm^2. We can see from Fig. 1 that Coils 2 and 3 will not receive the same power as Coil 1. The dimensions of the titanium case are 4.3 × 3.5 × 1 (cm) with a shell thickness of 0.25 mm, also shown in Fig. 1. The Rx coils are modelled inside a titanium case with a conductivity of 5.85× 10^5 (S/m) placed within the abdominal fat layer of the human body model shown in Fig. 2. The torso model is a round-corner rectangular cylinder with an overall size of 36 cm (width) by 40 cm (height) by 28 (depth).

The Tx coil will be located on the skin surface in front of the subcutaneous Rx coils to reduce the distance between the Tx and Rx. The single-turn circular planar Tx coil has a diameter D_{tx} = 5.28 cm. The transmitter coil is slightly larger than the receiving coils to tolerate misalignment conditions sufficiently.

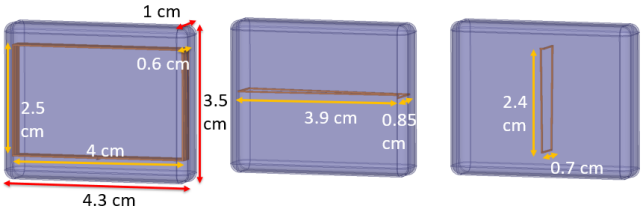

Fig. 1. (a) Coil 1 (facing the transmitter coil) 10 cm^2, (b) Coil 2 (horizontally faced) 3.31 cm^2, (c) Coil 3 (vertically faced) 1.68 cm^2.

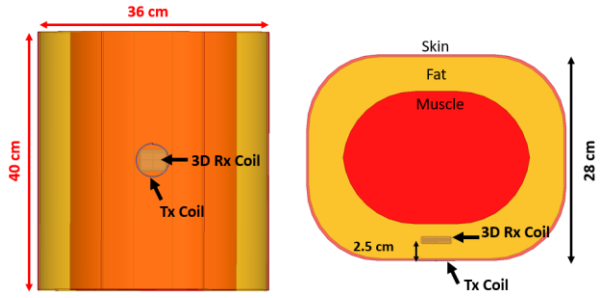

Fig. 2. Transmitter and 3D orthogonal receiver coils in the multi-layer tissue model: (a) Side view, (b) Top-down view.

The multi-layered cylinders consist of three different biological tissues: skin (external layer of thickness t_s = 0.3 cm), fat (intermediate layer of thickness t_f = 5 cm), and muscle (inner part). The dielectric properties at 40 kHz of the biological tissues are [20]:

Skin: ε_r = 1130, μ_r = 1, σ = 0.000249 (S/m);
Fat: ε_r = 197, μ_r = 1, σ = 0.0432 (S/m);
Muscle: ε_r = 11000, μ_r = 1, σ = 0.35 (S/m).

B. Metamaterial Lens

We explored incorporating a metamaterial lens into a wireless power transmission system to enhance further the system's magnetic field and power transfer efficiency [17]. The metamaterial lens design shown in Fig. 3(a) comprises a 5×5 unit cell arrangement with an FR4 substrate dimension of 20 cm × 20 cm × 0.16 cm. The metamaterial lens unit cell dimensions are 4 cm × 4 cm, shown in Fig. 3(b), with a square Split Ring Resonator (SRR) coil dimension of 3.2 cm × 3.2 cm, the copper coils have a width of 0.22 cm and a thickness of 0.02 cm. To maintain a compact structure at very low frequencies, a lumped capacitor is added to the SRR gap. The capacitance C is determine using $f = 1/\sqrt{LC}$ where f is the given frequency and L is the coil inductance calculated using the impedance values in High Frequency Structure Simulator (HFSS).

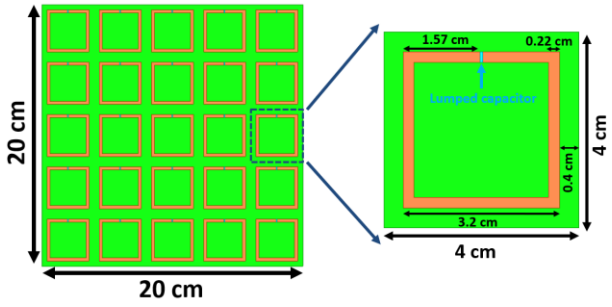

Fig. 3. Metamaterial Lens: (a) 5 by 5 unit cells (facing Tx) on FR4 substrate (green, facing Rx); (b) Details of one unit cell.

To accommodate the metamaterial lens, we move Tx away from the torso skin so that the lens can be placed between Tx and Rx. The separation distance betw H Field (A/m) d Tx coils is 7.4 cm (see Fig. 4). A 1-cm gap exists between the metamaterial lens and the skin's surface.

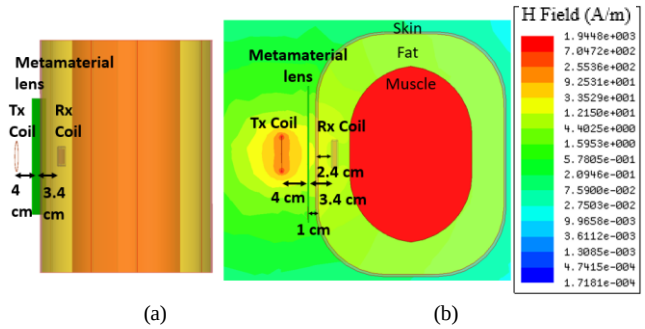

Fig. 4. Simulation model with metamaterial lens present: (a) Side view; (b) Top view.

III. Simulation Results

A. 3D Receiving Orthogonal Coils

We examine the performance of the 3D orthogonal receiver coils for three rotations around the three coordinate axes (±60° with a step of 30°) as shown in Fig. 5 [21]. The power received by each coil is recorded and the total power is the sum of these individual powers. Coil 1 has 10 turns (with an effective area of 100 cm^2) for all the cases.

Rotation 1: As shown in Fig. 5(a), the receiver coils are rotated around the y-axis. In this case the power received by Coil 2 can be ignored because its orientation (its normal direction) is always orthogonal to the Tx orientation. When the rotation angle increases, Coil 1 will receive less power while Coil 3 will receive more power. Since Coil 3 has 5 turns its effective area is 8.4 cm^2 which 8.4% of the effective area of Coil 1 with 10 turns. Thus, the power compensation by Coil 3 is much less than the power loss by Coil 1 when the rotation

angle increases. The simulation results show that Coil 3 with 5 turns contributes to a mere 1.4 dB to 2.6 dB to the total received power. When the number of turns of Coil 3 is increased from 5 to 15 turns, the area amounts to 25.2 cm^2, about 25.2% of the power transmitted through Coil 1 with 10 turns. Simulation results show that Coil 3 contributes between 1 dB to 4 dB increase in the total power transmitted compared to the power transmitted in Coil 1 with 10 turns alone.

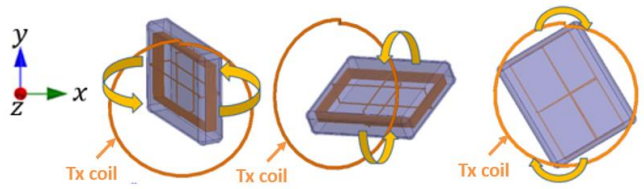

(a) (b) (c)

Fig. 5. Three rotations: (a) Rotation 1 around the *y*-axis, (b) Rotation 2 around the *x*-axis, and (c) Rotation 3 around the *z*-axis.

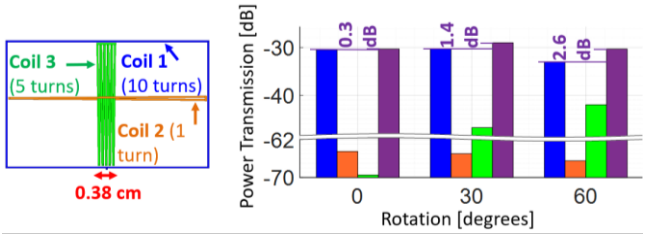

(a) (b)

Fig. 6. Coil 1: 10 turns, Coil 2: 1 turn, Coil 3: 5 turns: (a) Front view of 3D orthogonal coils, (b) Power Transmission as a function of Rotation 1.

Rotation 2: Fig. 5(b) shows the rotation of the receiver coils around the x-axis. In this case Coil 3 does not receive significant power while Coil 2 can compensate the power loss of Coil 1 when the rotation angle increases. With Coil 2 at 5 turns, its effective area is 16.55 cm^2 or 16.55% of that of Coil 1. It contributes between 1.9 dB to 4.3 dB to the total power transmitted compared to the power transmitted in Coil 1 with 10 turns alone (Fig. 7). The increased power transmission of Coil 2 at 5 turns compared to Coil 3 at 5 turns is due to Coil 2 having a larger effective area than Coil 3. When the number of turns of Coil 2 is increased to 15 turns, its effective area increases to 49.7 cm^2 and contributes 2 to 5 dB to the total power transmitted compared to the power transmitted in coil 1 with 10 turns alone.

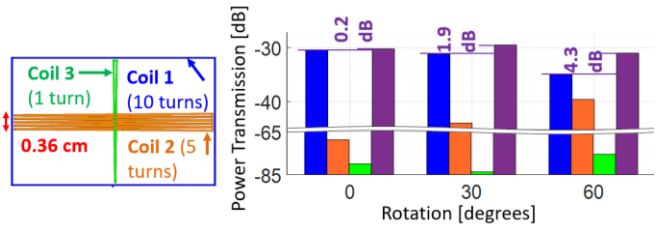

(a) (b)

Fig. 7. Coil 1: 10 turns, Coil 2: 5 turn, Coil 3: 1 turn: (a) Front view of 3D orthogonal coils, (b) Power transmission as a function of Rotation 2.

Rotation 3: Fig. 5(c) shows the receiver coils rotating around the z-axis. Note that this rotation does not change the orientation of Coil 1 (its normal direction) with respect to the Tx orientation. Also, the normal directions of Coils 2 and 3 are always perpendicular to the Tx orientation. Therefore, we expect no effect on the received powers. Our simulation results confirm the observation.

In those three rotations, the longer side of the titanium box is on the x-axis. We can examine the case when the longer side is on the y-axis. Now the roles of Coils 2 and 3 switch for each rotation. This means that Coil 2 will receive additional power under the effects of Rotation 1. In the same way, under the effects of Rotation 2, Coil 3 will receive additional power. Testing all coils with the same coil dimensions and number of turns, the 3D coils oriented vertically achieved similar results to the 3D coils oriented horizontally.

Lastly, we conducted a parametric study of increasing the number of turns in Coils 2 and 3 from 1 to 20. The results showed increases in power transfer efficiency when the height of these coils did not exceed 1/3 to 1/2 of the corresponding dimensions of the implantable unit. Exceeding these dimensions for Coils 2 and 3 resulted in interference between coils and reduced power transfer efficiency.

B. Effect of Metamaterial Lens

Using HFSS, we can find the inductance value of an SRR to be 71.6 nH from which the lumped capacitance value can be calculated as 221 μF. When the metamaterial lens is present as shown in Fig. 4, a 2 dB increase in total power transmission was achieved for all cases. The lens further mitigates the effects of rotation and increases the amount of power received by the 3D implantable device shown in Fig. 8 and Fig. 9.

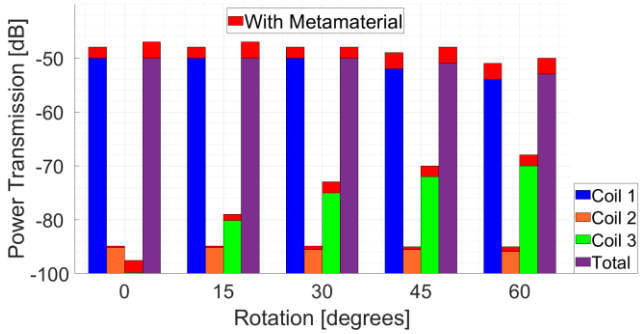

Fig. 8. Without metamaterial: Coil 1 (blue): 10 turns, Coil 2 (orange): 1 turn, Coil 3 (green): 15 turns, total power (purple); With metamaterial (Red). Power transmission as a function of Rotation 1.

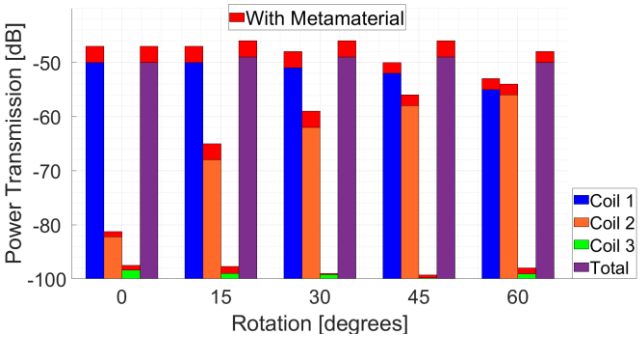

Fig. 9. Without metamaterial: Coil 1 (blue): 10 turns, Coil 2 (orange): 15 turns, Coil 3 (green): 1 turn, total power (purple); With metamaterial (Red). Power transmission as a function of Rotation 2.

C. SAR Calculations

Using HFSS, we can calculate the SAR values in tissues with their mass densities shown in Table I [22]. We focus on optimizing the number of turns for Coils 2 and 3 to maximize the power received while minimizing SAR values. Achieving similar results dependent on receiver orientation, we tested four Rx cases for Rotations 1 and 2 with 1W of Tx power to examine the effects on SAR values and power transmission shown in Fig. 10.

The single-coil receiver case is our reference case, shown in Fig. 10(a). In the 3D receiver cases, we tested 1 turn, 5 turns, and 10 turns for coils 2 and 3, shown in Fig. 10(b), (c), and (d). For all cases, Coil 1 remains at 10 turns, and the location of the transmitter and the receivers were placed at the same distances as Fig. 4. The SAR calculations were tested at 0° and 10° for both rotations. At the same time, power transmission was tested at 0° to 60° for both rotations. Since HFSS calculated similar average SAR values for Rotations 1 and 2, the data for Rotation 2 has been omitted. Our results showed that increasing the number of turns does not significantly increase SAR values for Rotation 1, shown in Table II. However, in Fig. 11 and 12, increasing the number of turns for Coils 2 and 3 in both rotations causes power transmission interference to Coil 1, which lowers the total power received.

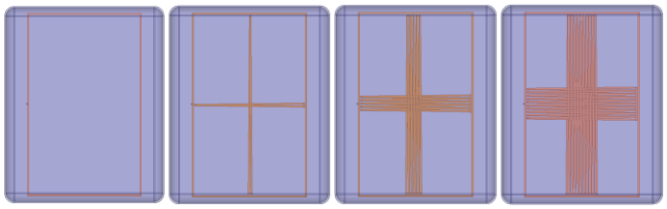

(a) (b) (c) (d)

Fig. 10. Vertically-faced 3D Rx cases: (a) Coil 1: 10 turns, (b) Coil 1: 10 turns, Coil 2: 1 turn, Coil 3: 1 turn, (c) Coil 1: 10 turns, Coil 2: 5 turns, Coil 3: 5 turns, (d) Coil 1: 10 turns, Coil 2: 10 turns, Coil 3: 10 turns:

TABLE I
MASS DENSITY VALUES FOR TISSUE

Skin ρ (kg/m^3)	Fat ρ (kg/m^3)	Muscle ρ (kg/m^3)
Skin = 1109	Fat = 911	Muscle = 1090

TABLE II
SAR VALUES FOR VERTICALLY-FACED RX AS A FUNCTION OF ROTATION

SAR Location	1D Receiver (reference) (W/kg)	Coil 1: 10 turns Coil 2: 1 turn Coil 3: 1 turn (W/kg)	Coil 1: 10 turns Coil 2: 5 turns Coil 3: 5 turns (W/kg)	Coil 1: 10 turns Coil 2: 10 turns Coil 3: 10 turns (W/kg)
Power	**1W**	**1W**	**1W**	**1W**
Skin	6.4e-11	6.8e-11	6.4e-11	6.7e-11
Muscle	5.5e-9	5.7e-9	5.5e-9	5.5e-9
Fat	2.2e-9	2.3e-9	2.2e-9	2.2e-9

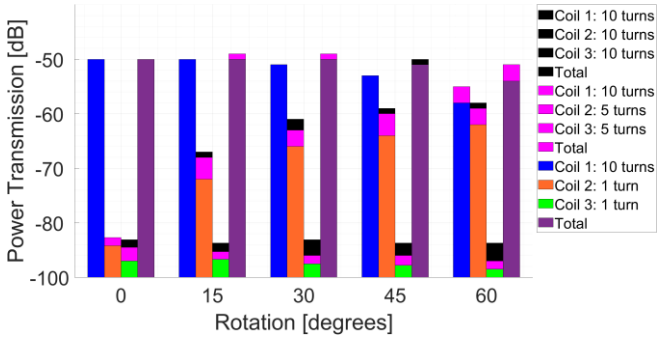

Fig. 11. Vertically-faced 3D Rx power transmission as a function of Rotation 1.

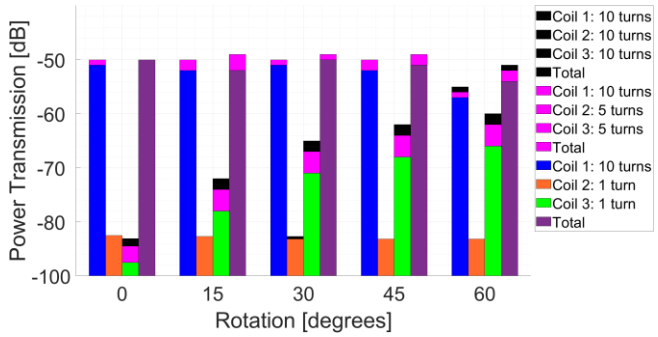

Fig. 12. Vertically-Faced 3D Rx power transmission as a function of Rotation 2.

IV. CONCLUSION

In summary, the simulation results showed that implementing the three-coil arrangement in the implantable devices mitigates rotation effects. In some cases, it was observed that the inclusion of three orthogonal coils increased the total power received by 15% in the implantable unit. The three-coil arrangement and associated increase in power transmission efficiency may also enable a lower-powered transmitter coil, thus lowering the risk of tissue absorption within the human body. The three-coil arrangement achieves similar SAR values to the conventional single-coil receiver. Clearly, increasing the number of turns in each coil will increase the received power in the implantable unit. However, our simulation study on the number of turns for Coils 2 and 3 shows that limiting the number of turns in each coil to 10 is optimal as it reduces weight and interference between coils. Additionally, using a metamaterial lens tuned to meet set frequencies in commercially available implantable devices improved power transmission efficiency by 2 dB at the expense of increased SAR values in the skin and fat layers. Future development includes further examining the effectiveness of metamaterial uses to enhance power transmission while minimizing SAR increase, reexamining the optimum frequency band for implantable devices for effective use of implantable medical devices, and validating all results experimentally.

REFERENCES

[1] S. R. Khan, S. K. Pavuluri, G. Cummins, and M. P. Desmulliez, "Wireless power transfer techniques for Implantable Medical Devices: A Review," *Sensors*, vol. 20, no. 12, pp. 10-20, Jun. 2020

[2] Z. Zhang and B. Zhang, "Angular-Misalignment Insensitive Omnidirectional Wireless Power Transfer," *IEEE Trans. Ind. Electron.*, vol. 67, no. 4, pp. 2755–2764, Apr. 2020, doi: 10.1109/TIE.2019.2908604.

[3] H. Hu, W. Xu, Y. Shen, and Y. Li, "A Planar Orthogonal Receiver for Multi-degree of Freedom Wireless Power Transfer," in *2022 IEEE International Conference on Artificial Intelligence and Computer Applications (ICAICA)*, Dalian, China, Jun. 2022, pp. 1027–1031. doi: 10.1109/ICAICA54878.2022.9844638.

[4] W. M. Ng, C. Zhang, D. Lin, and S. Y. Ron Hui, "Two- and Three-Dimensional Omnidirectional Wireless Power Transfer," *IEEE Trans. Power Electron.*, vol. 29, no. 9, pp. 4470–4474, Sep. 2014, doi: 10.1109/TPEL.2014.2300866.

[5] J. P. W. Chow, N. Chen, H. S. H. Chung, and L. L. H. Chan, "An Investigation Into the Use of Orthogonal Winding in Loosely Coupled Link for Improving Power Transfer Efficiency Under Coil Misalignment," *IEEE Trans. Power Electron.*, vol. 30, no. 10, pp. 5632–5649, Oct. 2015, doi: 10.1109/TPEL.2014.2374651.

[6] W. Tang, Q. Zhu, J. Yang, D. Song, M. Su, and R. Zou, "Simultaneous 3-D Wireless Power Transfer to Multiple Moving Devices With Different Power Demands," *IEEE Trans. Power Electron.*, vol. 35, no. 5, pp. 4533–4546, May 2020, doi: 10.1109/TPEL.2019.2942098.

[7] Z. Zhang, S. Zheng, Z. Yao, D. Xu, P. T. Krein, and H. Ma, "A Coil Positioning Method Integrated With an Orthogonal Decoupled Transformer for Inductive Power Transfer Systems," *IEEE Trans. Power Electron.*, vol. 37, no. 8, pp. 9983–9998, Aug. 2022, doi: 10.1109/TPEL.2022.3155270.

[8] G. Lipworth *et al.*, "Magnetic Metamaterial Superlens for Increased Range Wireless Power Transfer," *Sci Rep*, vol. 4, no. 1, p. 3642, Jan. 2014, doi: 10.1038/srep03642.

[9] B. Wang, K. H. Teo, T. Nishino, W. Yerazunis, J. Barnwell, and J. Zhang, "Experiments on wireless power transfer with metamaterials," *Appl. Phys. Lett.*, vol. 98, no. 25, p. 254101, Jun. 2011, doi: 10.1063/1.3601927.

[10] A. L. A. K. Ranaweera, C. A. Moscoso, and J.-W. Lee, "Anisotropic metamaterial for efficiency enhancement of mid-range wireless power transfer under coil misalignment," *J. Phys. D: Appl. Phys.*, vol. 48, no. 45, p. 455104, Nov. 2015, doi: 10.1088/0022-3727/48/45/455104.

[11] A. L. A. K. Ranaweera, T. P. Duong, and J.-W. Lee, "Experimental investigation of compact metamaterial for high efficiency mid-range wireless power transfer applications," *Journal of Applied Physics*, vol. 116, no. 4, p. 043914, Jul. 2014, doi: 10.1063/1.4891715.

[12] T. S. Pham, A. K. Ranaweera, V. D. Lam, and J.-W. Lee, "Experiments on localized wireless power transmission using a magneto-inductive wave two-dimensional metamaterial cavity," *Appl. Phys. Express*, vol. 9, no. 4, p. 044101, Apr. 2016, doi: 10.7567/APEX.9.044101.

[13] S. Lee *et al.*, "High Efficiency Wireless Power Transfer System using a Two-stack Hybrid Metamaterial Slab," in *2019 IEEE Wireless Power Transfer Conference (WPTC)*, London, United Kingdom, Jun. 2019, pp. 616–619. doi: 10.1109/WPTC45513.2019.9055525.

[14] J. Liu, Z. Chen, J. Zhou, and H. Sun, "Compact Triplex-layer Metamaterials Design for Wireless Power Transfer Efficiency Enhancement," in *2020 IEEE 19th Biennial Conference on Electromagnetic Field Computation (CEFC)*, Pisa, Italy, Nov. 2020, pp. 1–4. doi: 10.1109/CEFC46938.2020.9451226.

[15] D. Shan, H. Wang, K. Cao, and J. Zhang, "Wireless power transfer system with enhanced efficiency by using frequency reconfigurable metamaterial," *Sci Rep*, vol. 12, no. 1, p. 331, Jan. 2022, doi: 10.1038/s41598-021-03570-8.

[16] W. Lee and Y.-K. Yoon, "Tunable Metamaterial Slab for Efficiency Improvement in Misaligned Wireless Power Transfer," *IEEE Microw. Wireless Compon. Lett.*, vol. 30, no. 9, pp. 912–915, Sep. 2020, doi: 10.1109/LMWC.2020.3015680.

[17] I. V. Soares, F. M. Freitas, and U. C. Resende, "Efficiency Enhancement in Mid-Range RWPT Systems by GRIN Metasurface Lenses," in *2021 IEEE Wireless Power Transfer Conference (WPTC)*, San Diego, CA, USA, Jun. 2021, pp. 1–4. doi: 10.1109/WPTC51349.2021.9458020.

[18] T. Campi, S. Cruciani, F. Maradei, A. Montalto, F. Musumeci, and M. Feliziani, "EMI in a Cardiac Implantable Electronic Device (CIED) by the Wireless Powering of a Left Ventricular Assist Device (LVAD)," *IEEE Trans. Electromagn. Compat.*, vol. 63, no. 4, pp. 988–995, Aug. 2021, doi: 10.1109/TEMC.2020.3047465.

[19] Y. Jia *et al.*, "Position and Orientation Insensitive Wireless Power Transmission for EnerCage-Homecage System," *IEEE Trans. Biomed. Eng.*, vol. 64, no. 10, pp. 2439–2449, Oct. 2017, doi: 10.1109/TBME.2017.2691720.

[20] "Dielectric Properties » IT'IS Foundation." https://itis.swiss/virtual-population/tissue-properties/database/dielectric-properties/ (accessed Aug. 24, 2022).

[21] B. Wong, S. Clemens, M. F. Iskander, and Z. Yun, "Improvement of Wireless Power Transmission Efficiency to Implantable Devices," in *2022 IEEE International Symposium on Antennas and Propagation and North American Radio Science Meeting*, 2022.

[22] "Density » IT'IS Foundation." https://itis.swiss/virtual-population/tissue-properties/database/density/ (accessed Jun. 13, 2023).